Desalination and Water Treatment
www.deswater.com
doi: 10.5004/dwt.2020.26370

206 (2020) 133–143
December

Thermodynamics of sub-atmospheric vapor pipeline (SAVP) for seawater desalination: a study for vapor-liquid equilibrium and the fluid properties associated with a field application

Mona Shojaei[a], Mohsen Nosrati[b,*], Reza Attarnejad[c], Bahram Saghafian[a]

[a]*Department of Civil Engineering, Science and Research Branch, Islamic Azad University, Tehran, Iran, Tel. (+98) 21-4486-8540; emails: shojaei.mon@gmail.com (M. Shojaei), b.saghafian@gmail.com (B. Saghafian)*
[b]*Biotechnology Group, Chemical Engineering Department, Tarbiat Modares University, P.O. Box: 14115-143, Tehran, Iran, Tel. (+98) 21-8288-4372; email: mnosrati20@modares.ac.ir (M. Nosrati)*
[c]*School of Civil Engineering, College of Engineering, University of Tehran, Tehran, Iran, Tel. (+98) 21-6111-2225; email: attarnjd@ut.ac.ir (R. Attarnejad)*

Received 4 September 2019; Accepted 23 July 2020

ABSTRACT

In this paper, equilibrium thermodynamics of sub-atmospheric vapor pipeline (SAVP), that is, one of the seawater desalination methods is analyzed in theory and application in a natural field. SAVP occurs based on the temperature difference between a warm source and a cold environment. The energy consumption for this method is close to zero and has great potential for large-scale applications. However, for this method, there is no thermodynamic analysis and formulations including calculations of energies, entropy estimation, temperature profiles, and the most important issue, that is, determination of pressure drop (which is the main motivation of vapor transfer), in scientific sources. Fluid unknowns including $T(x)$, $P(x)$, $V(x)$, and $\rho(x)$ are computed and recorded using momentum equations, continuity, and an appropriate equation of estate by adopting small spacing lengths along the pipe lane. All thermodynamic functions (ΔU, ΔH, ΔG, ΔA, and ΔS) and fluid properties along with the vapor transfer velocity and vapor pressure drop will be determined by the basic thermodynamic relations, Maxwell's, Gibbs–Helmholtz's, and Clausius' equations. The outputs of this analysis are presented in a real and natural field within 30 km of a warm source (Bandar Abbas) and a cold source (Geno Heights) with an elevation of 2,300 m.

Keywords: Sub-atmospheric vapor pipeline (SAVP); Seawater desalination; Vapor-liquid equilibrium (VLE); Thermodynamics; Fluid properties

1. Introduction

The principles of seawater desalination are based on energy consumption and the separation of freshwater from salty water. Therefore, in the field of seawater desalination, topics such as energy conversions, energy efficiency, entropy generation, phase equilibriums, streams' properties, and system stability are also directly related to the science of thermodynamics [1–4]. In industry, seawater desalination is performed by thermal and membrane methods widely [5]. The thermal methods for desalination include multi-effect distillation (MED) and multi-stage flash (MSF), while the most common membrane desalination method is reverse osmosis (RO), that the required energy to produce each cubic meter of freshwater from salinity waters has been calculated, tested, and determined [6]. Thermodynamic topics of thermal methods include the determination of phase change heat, mass equilibrium, phase equilibrium, and non-ideal properties of liquid and vapor phases which are directly related to the salinity of the raw water. Of course, issues such as solubility and release of dissolved gases in seawater and economic discussion of corrosion control in process equipment

* Corresponding author.

especially heat exchangers, columns, and mass transfer trays, are also important [7,8].

The non-ideal thermodynamic interpretation of saline water is related to the activity coefficients of the soluble components (γ) and is usually expressed by the mean salt activity coefficient ($\gamma^{\pm}$) or the water osmotic coefficient (ϕ) [1]. Numerous thermodynamic issues have been proposed for the design of MED and MSF and the reduction of power consumption in RO as well as the entropy studies [9–11]. Generally, the thermodynamics of seawater desalination in one hand tries to minimize energy consumption and on the other hand, seeks the knowledge could provide a better understanding of entropy minimization (ΔS) [12]; these, however, lead the design of equipment in desalination industries to be performed and implemented in its best feature.

Apart from the membrane-based desalination (which is not the focus of this paper's research), thermal desalination still needs more thermodynamic interpretations. In the meantime, Maxwell's equations and equation of estates (EOS) which explain the non-ideality of the vapor phase, together with the Gibbs–Dühem (G–D) and Gibbs–Helmholtz equations, enable us to determine the thermodynamic energies, that is, ΔU, ΔH, ΔG, and ΔA in a thermal desalination system. However, phase equilibrium equations such as Antoine's equation that relate temperature and pressure of the equilibrium phases can also facilitate the calculation process by eliminating one or more unknowns [13].

SAVP method is proposed already [14,15] and by vapor transfer with a natural force (which is the inherent temperature difference between the warm and cold sources), provides vapor transmission, and its condensation at the cold source. This method, on a large scale, can transfer vapor from the warm coastal waters of the ocean to adjacent cold heights (mountains) and enables us to achieve freshwater in the highlands without energy consumption followed by the possibility of free water distribution or even use of power-generating turbines. Vapor transfer, on a smaller (but more effective) scale, can transform the wastewater of a hotel or industrial or tourism town on top of a tower or building into freshwater with the potential for having the freshwater at elevation. Taking into account all the positive and favorable factors, wastewater can be used instead of seawater for desalination. The wastewater, on the one hand, is less saline than seawater, and on the other hand, it has higher temperatures (usually), both of which make it easier to desalinate compared to the seawater. Therefore, small-scale vapor transfer can be more practical and economical. A vacuum pump is used to start the vapor transfer (only once). The vapor moves through the pipe and reaches the cold source. Due to the large reduction in the volume of the fluid in the condensation part, a natural vacuum occurs and the vapor is automatically transferred and there is no longer any need for energy to provide the vacuum. It should be noted that the pressure difference in the condensation part defined by the Clapeyron equation is the main stimulator of the cold vapor transfer and can technically support the industrial design of such desalination.

Interpretation and discussion of thermodynamic variables in the transfer pipeline, including thermodynamic energies (U, H, G, and A) and variables of the Maxwell equations (S, T, P, and V) in the SAVP method have not been addressed and reviewed in the literature for such desalination. These interpretations and the pressure and temperature drop are discussed in this study along with the determination of the fluid velocity and the mass flow rate of the vapor transferred as well as the fundamentals of designing heat and mass exchangers. The results of this study can provide the preliminaries for unsteady vapor transfer in which the time variable is involved. In a more advanced state, the results of this study can be used for the non-equilibrium thermodynamics (NET) of vapor transfer (which requires different investigations and research).

2. Methods

2.1. Thermodynamics of SAVP method

Sub-atmospheric vapor pipeline (SAVP) issue needs a thermodynamic background to explain the heat and mass transfer relations. Along the pipeline route, both at a macro level such as performed by previous researchers [14,15] or at a commercial scale such as the recycling of the sewage of a commercial complex and converting it into distilled water, the pattern of pressure and temperature changes throughout the route must be clearly identified, so that the necessary engineering works such as insulation, heat transfer, minimization of heat dissipation, determination of the fluid state (physical state including vapor or liquid) along the entire route, etc., are performed. Therefore, the only way to achieve this goal is to determine the thermodynamic properties of the fluid throughout the route. SAVP consists of three stages including evaporation, vapor motion, and condensation at the final point. In this process, determination of the thermodynamic properties of the fluid is directly related and limited to only the vapor transfer section, because the initial stage (warm source) and the final stage (cold source) of this transfer involve saturated fluid transfer; therefore, their thermodynamic properties can be extracted from the vapor and saturated liquid thermodynamic tables.

2.2. Relationship between variables and thermodynamic functions with SAVP method

In addition to the determination of $T(x)$ and $P(x)$, both of which are functions of the transfer location (inside the pipe), other thermodynamic functions must also be determined based on the changes in the distance (x). Determination of these thermodynamic properties leads to the determination of basic functions such as the fluid enthalpy (H), fluid Gibbs energy (G), internal energy (U), and Helmholtz energy (A) that directly involves and specifies the four thermodynamic variables including temperature (T), pressure (P), volume (V), and entropy (S). As mentioned earlier, the fluid can be considered as saturated or in general thermodynamic equilibrium only at the vapor generation point (the beginning of the route or at the evaporator site) and at the condensation point (the end of the path or at the condenser site). The thermodynamic tables can be directly used to determine the energies and thermodynamic parameters; however, the fluid transferred along the pipeline route is not in equilibrium with the liquid, in other words, not saturated, and is

practically considered to be as the hot vapor. Thus, a scientific and engineering approach for the designer of the SAVP is needed to accurately determine the thermodynamic properties of the fluid. The aim of this study is to specify and quantify the thermodynamic functions and relations in the sub-atmospheric vapor transfer technology along the route.

2.3. Method of calculation of variables in SAVP method

The temperature difference between the origin and the destination is the main cause of the vapor transfer that flows as hot vapor through the pipe. The pipe is assumed to be insulated until the condensation begins. The general assumption in the calculation of the thermodynamic variables by the SAVP method is that using the momentum and continuity equations and a proper equation of state with small spaced intervals along the path, the fluid unknowns including $T(x)$, $P(x)$, $V(x)$, and $\rho(x)$ are computed and recorded in each element. The computations are performed in two stages. For an initial assumption and reduction of unknowns, in the first step, the fluid is considered as a saturated vapor and an ideal gas and the fluid temperature and pressure are calculated up to a distance of 30 km (a distance of the warm source (Bandar Abbas) to the cold source (Geno heights)) and the altitude difference of 2,300 m. Then, in the second step, to obtain the actual behavior of the fluid in the pipe, the vapor is considered as a hot vapor and the non-ideal gas state equation is regarded. The algorithm presented in Fig. 1 and Eqs. (1) (momentum), (2) (continuity), and (3) (state equation for an ideal gas) are considered for

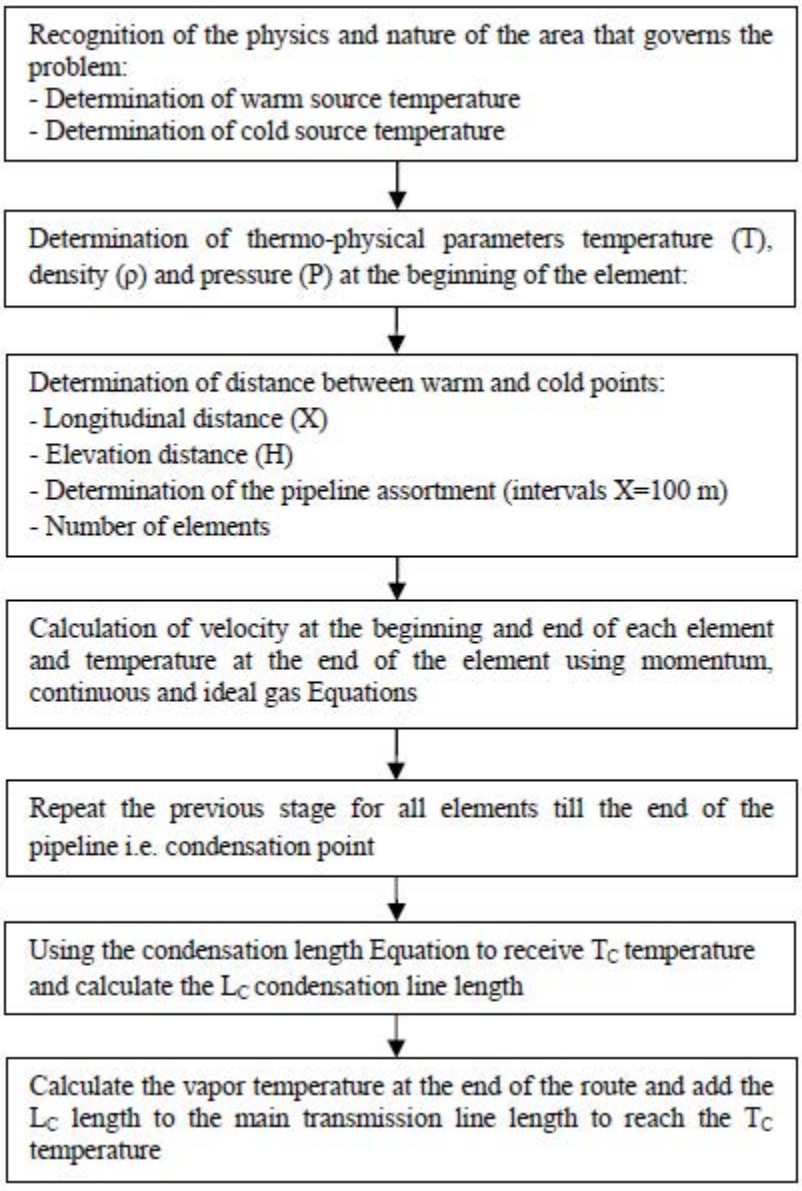

Fig. 1. Elemental calculation algorithm for calculating temperature, pressure, and velocity in the process of desalination by SAVP method.

the calculations. In other words, it can be said that the first stage, in a way, is a hypothetical approach to simplify, and the second stage shows the actual solution of the problem, which matches its nature.

$$\left(\rho_1-\rho_2\right)u^2+\left(P_1-P_2\right)+\rho_2 gL\cdot\sin\left(\alpha\right)+\frac{2fl}{D}\rho_2u^2=0 \quad (1)$$

$$\rho_1u_1=\rho_2u_2 \quad (2)$$

$$PV=nRT\rightarrow Pnv=nRT\rightarrow\frac{P}{\rho_t}=RT\rightarrow P=\frac{\rho}{18}RT \quad (3)$$

This algorithm lacks trial and error and assumes that the fluid is as the saturated vapor throughout the route. However, what is actually happening is that the fluid leaves the warm source in the saturated state and travels the entire length of the transfer path as unsaturated or hot vapor due to the pressure drop to reach the condensation point. According to the principles of the SAVP desalination method, the condensing system itself is a non-insulated pipe in which the condensation operation is performed gradually and has a definite, calculable length as L_C [13] and the conditions of the vapor saturation and its change to liquid starts from there. The vapor quality (usually denoted by x) is equal to one at the beginning of the condensation length and is zero at the end of this length in which the entire vapor is converted to liquid. The vapor quality decreases from one to zero during the passage from the condensation length L_C, and the fluid moves in this path in a two-phase state. This is illustrated in Fig. 2. The curve shown in this figure is the saturation curve, with the upper and lower parts being the vapor phase (V) and the liquid phase (L), respectively. On the curve, the saturated vapor phase and the liquid phase interact and are in equilibrium. In practice, the thermodynamic conditions at the beginning of the path (evaporator) and the end of the path (condenser) are such that in terms of temperature and pressure, the two liquid and vapor phases are located on this curve, but the vapor transferred along the pipe certainly lays in the hot vapor zone.

The logic behind connecting and adding the L_C length to the transfer length is that the designer is sure that from this point on, the vapor quality (x) will slowly decrease from one to zero. The L_C length is designed and installed as inclined

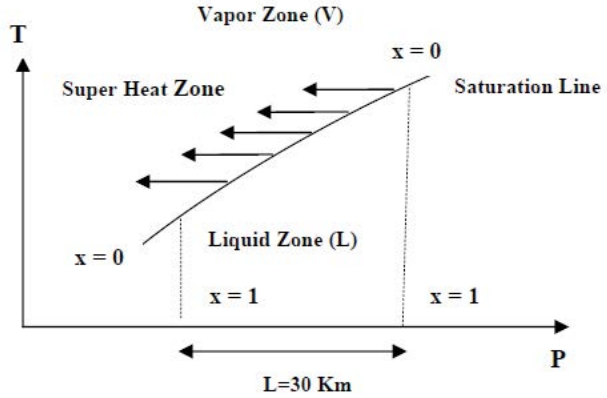

Fig. 2. Vapor quality changes in the saturation curve and the location of vapor transport conditions in the hot vapor zone that pressure lower than the saturation pressure and a temperature higher than the saturation temperature.

with a small slope. Fig. 3a demonstrates the vapor quality changes as described above. Reaching the zero vapor quality requires traveling a distance and, as the asymptote of the curve in the right section of Fig. 3a shows requires a certain length of pipe. Fig. 3b will be achieved if the average saturated vapor quality (0.5) in the condensation length is considered as the base or operational quality. The number 0.5 is the average of one and zero. This is a practical and acceptable estimate based on the references used and estimated the L_C length [14] with the average quality (0.5).

These assumptions and calculations lead to obtaining the fluid temperatures $T(x)$ assuming the fluid movements, these temperatures are shown as horizontal arrows in Fig. 2. Actual pressures $P(x)$, of course, do not lay on the TP temperature–pressure (saturation) line. These pressures are usually lower than the saturation pressure, which lay on the left-hand side of the saturation line in accordance with the arrow direction. The actual pressures are obtained using a real gas state equation such as the van Der Waals equation instead of the ideal gas equation.

2.4. State equation and thermodynamic functions

The van Der Waals state equation is introduced in Eq. (4). This equation applies an increasing correction to pressure (P) and a decreasing correction to volume (V) on

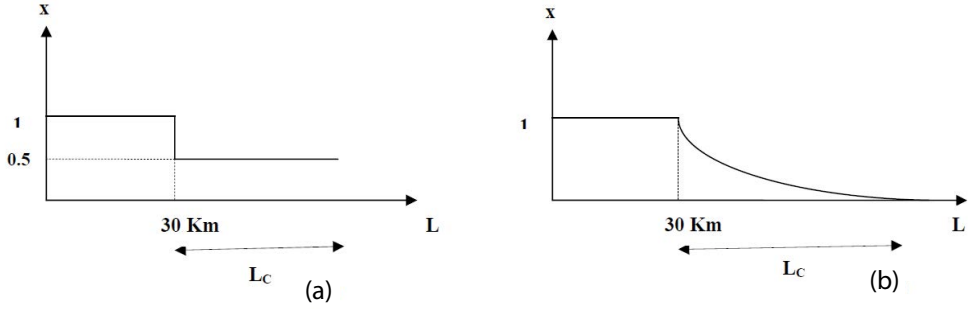

Fig. 3. Vapor quality changes based on assumptions (a) gradual decline in vapor quality from the beginning of the condensation point and (b) reduction of vapor quality to average (0.5).

the ideal gas pattern, which correspond, respectively, to molecules that do not only apply pressure on the container wall but also to each other (or diverge from each other) and subsequently the volume (V) decreasing correction corresponds to the pure volume of gas molecules that must be subtracted from the total volume of gas dispersion. The term gas is here referred to as the transferable vapor. The van Der Waals equation is written as follows.

$$\left(P+\phi_1\right)\left(V+\phi_2\right)=nRT \tag{4}$$

where ϕ_1 is associated with the pressure that the gas molecules apply on each other and this differs from the pressure that the molecules enter the container wall. ϕ_2 is also related to the volume of the gas itself and differs from the volume that the gas occupies. Usually, the actual pressure is greater than what is measured and the actual volume is less than what is occupied. Therefore, the van der Waals' equation can be written as Eqs. (5) and (6).

$$\left(P+\alpha\right)\left(V-\beta\right)=nRT,\ \alpha,\beta>0 \tag{5}$$

$$\left(P+\frac{n^2a}{V^2}\right)\left(V-nb\right)=nRT \tag{6}$$

If the van Der Waals equation is written as a pressure-explicit equation, it will become as Eq. (7).

$$P=\frac{nRT}{V-nb}-\frac{n^2a}{V^2} \tag{7}$$

where T, P, and V are the vapor temperature (in K), the vapor pressure (in bars), and the vapor volume in the pipe segment (in L), respectively; moreover, a and b are the parameters of the van Der Waals equation that differ depending on the material and can be extracted from the thermodynamic tables and texts and their units should be given special attention. The volume of the pipe segments, the number of vapor moles, the relationship between the thermodynamic density and the fluid density, the gas constant, and the values of the van Der Waals equation for vapor are given in Eqs. (8a)–(8d).

$$V_p=\frac{\pi D^2}{4}L \tag{8a}$$

$$n=\frac{m}{M_w}=\frac{m}{18}=\frac{\rho_t V_p}{18} \tag{8b}$$

$$\rho_t=\frac{\rho}{18} \tag{8c}$$

$$a=5.537\left(\frac{\left(\text{bar L}^2\right)}{\text{mol}^2}\right),\quad b=0.03049\left(\frac{\text{L}}{\text{mol}}\right),\quad R=0.083144\left(\frac{\text{bar L}}{\text{K}}\right) \tag{8d}$$

A logical relationship between the mentioned energies (U, H, G, and A) and the thermodynamic variables (T, P, V, and S) has been provided by the Maxwell relations to the engineering fields so that in any given situation, as necessary, link these energies to the four thermodynamic variables and find the unknowns. In the event of drastic changes in temperature at the origin and destination, a NET discussion will arise that can subsequently be studied independently.

3. Results and discussion

3.1. Hot vapor, state equation, and Maxwell equations

A thermodynamic discussion is usually started with the four main energies as Eqs. (9)–(12). According to the calculations of the algorithm of Fig. 1, temperature and pressure both decrease along the path from the warm source to the beginning of the cold source (where the fluid is still transferred as vapor and the vapor quality is equal to (x = 1)).

$$U=U\left(S,V\right) \tag{9}$$

$$H=H\left(S,P\right) \tag{10}$$

$$A=A\left(V,T\right) \tag{11}$$

$$G=G\left(T,P\right) \tag{12}$$

The ideal gas assumption hinders calculations of changes in thermodynamic functions and all variations of these functions are assumed as zero. On the other hand, the assumption of the fluid movement throughout the path as the saturated vapor until the beginning of the condenser length is not a convincing assumption. The temperatures calculated from the algorithm of Fig. 1 can lead to movement of the fluid as a hot vapor to the beginning of the condenser with pressures other than saturation pressure, and of course lower than that, which is a real and natural case. Therefore, a well-known and low-error state equation such as the van Der Waals equation is used to calculate the actual pressures that provide both the actual gas (vapor) and its unsaturated state. Now, the cold vapor transfer operational line is differentiated from the saturation line, and the magnitude of the difference between them (the area between the saturation curve and the fluid flow line as the hot vapor) at any temperature and pressure can be the source of calculation of the thermodynamic functions. Fig. 4 contains two basic curves, one showing the saturation curve and the other showing the fluid flow line as the hot vapor through the pipe. According to Fig. 4, the SAVP method, which occurs in the hot vapor path, has a higher temperature at constant pressure than the saturation path and has a lower pressure at the constant temperature.

Changes in the total basic energies from Eqs. (9)–(12) are followed by Eqs. (13)–(16).

$$dU=TdS-PdV \tag{13}$$

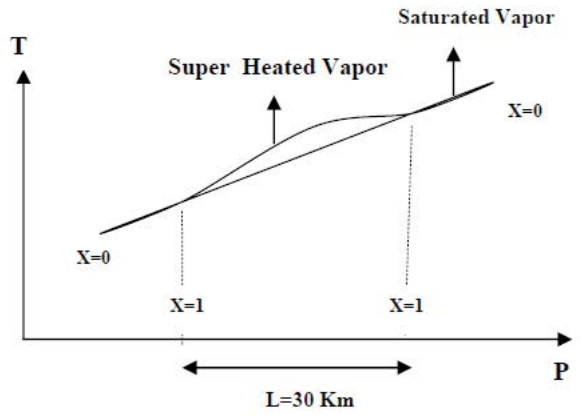

Fig. 4. Temperature and pressure changes in the process of desalination by SAVP method in two saturated and super heated vapor paths.

$$dH = TdS + Vd \tag{14}$$

$$dA = SdT - PdV \tag{15}$$

$$dG = VdP - SdT \tag{16}$$

From the basic energy Eqs. (13)–(16), it can be noticed that the Gibbs energy G is of particular importance because of its direct dependence on the two measurable parameters T and P and can be the origin of calculations for other energies and other parameters. This means that in the engineering field, because of the independence of T and P of the system's mass, they can be easily measured by measuring devices. Volume (V) is easily computable for the pre-engineered systems, but for open and unknown systems it should be computed as an unknown. The entropy S is a variable for which there are no measuring instruments and should only be determined by calculations. Therefore, after the temperature and pressure are readily measured, the volume (V), and especially the entropy (S) must be determined or calculated. In the SAVP thermodynamics, given the specified and closed system, the volume (V) can be conceived as a known parameter. Therefore, the only definite thermodynamic unknown that must be computed is the entropy (S). To calculate unknown variables (such as S) from known parameters, the Maxwell relations are used.

$$\left(\frac{\partial S}{\partial V}\right)T = \left(\frac{\partial P}{\partial T}\right)V \tag{17}$$

$$\left(\frac{\partial V}{\partial T}\right)P = -\left(\frac{\partial S}{\partial P}\right)T \tag{18}$$

$$\left(\frac{\partial T}{\partial P}\right)S = \left(\frac{\partial V}{\partial S}\right)P \tag{19}$$

$$\left(\frac{\partial P}{\partial S}\right)V = -\left(\frac{\partial T}{\partial V}\right)S \tag{20}$$

The following couple and highly used equations can also be derived from the Maxwell equations and the basic energy equations.

$$\left(\frac{\partial U}{\partial S}\right)V = T \quad \left(\frac{\partial U}{\partial V}\right)S = -P \tag{21}$$

$$\left(\frac{\partial H}{\partial S}\right)P = \mathrm{T} \quad \left(\frac{\partial H}{\partial P}\right)S = V \tag{22}$$

$$\left(\frac{\partial A}{\partial V}\right)T = -P \quad \left(\frac{\partial A}{\partial T}\right)V = -S \tag{23}$$

$$\left(\frac{\partial G}{\partial P}\right)T = V \quad \left(\frac{\partial G}{\partial T}\right)P = -S \tag{24}$$

The importance of the Gibbs energy (G) and its main variables in calculating the thermodynamic unknowns discussed above is totally clear in Eq. (24). The best thermodynamic equations that can be applied to determine the unknowns (while directly using the Maxwell equations) are the state equations. The van Der Waals equation is used as a suitable state equation (as introduced earlier). The terms n^2a/V^2 and nb are the increasing pressure correction and the decreasing volume correction, respectively.

3.2. Determination of basic energies and entropy

To determine the four basic energies in thermodynamics (U, H, G, and A) and the process of their calculation using the Maxwell equations, the internal energy U is first determined and then the enthalpy H of the system is calculated. According to the Gibbs–Helmholtz equation, the Gibbs energy G can be determined by deriving the term G/T relative to temperature at the constant pressure. To determine the Helmholtz energy A, the entropy S must first be determined and then the internal energy can be obtained. The process of determining the basic energies for the SAVP method is discussed below. The specific heat of vapor at constant pressure C_P and at the constant volume C_V are obtained through the determination of the two basic energies H and U and their variations with respect to the temperature changes. The calculation of these specific heats as stated above is only valid when they are determined for each pipe segment and to determine their overall value, these values must be certainly averaged or integrated throughout the pipe.

3.2.1. Determination of internal energy U

The first energy obtained by the van Der Waals equation and the helpful Maxwell equations is the internal energy U, the process of determination of which is presented below. Eq. (25), the basic equation for determining the internal energy of U, has been used first.

$$dU = TdS - PdV \tag{25}$$

From which (after dividing the sides of the equation by dV), the following equations are obtained.

$$\left(\frac{dU}{dV}\right)T = T\left(\frac{dS}{dV}\right)T - P \tag{26}$$

or

$$\left(\frac{\partial U}{\partial V}\right)T = T\left(\frac{\partial S}{\partial V}\right)T - P \tag{27}$$

The term $\left(\frac{\partial S}{\partial V}\right)T$ is an unknown that could be obtained by the Maxwell equation and the van Der Waals equation through Eqs. (28)–(30).

$$\left(\frac{\partial S}{\partial V}\right)T = \left(\frac{\partial P}{\partial T}\right)V \tag{28}$$

$$P = \frac{nRT}{V - nb} - \frac{n^2 a}{V^2} \tag{29}$$

$$\left(\frac{\partial P}{\partial T}\right)V = \frac{nR}{V - nb} \tag{30}$$

So,

$$\left(\frac{\partial U}{\partial V}\right)T = \frac{nRT}{V - nb} - \frac{nRT}{V - nb} + \frac{n^2 a}{V^2} \tag{31}$$

Finally, the changes in the internal energy U are calculated by changing the volume of fluid at constant temperature through Eq. (32).

$$\left(\frac{\partial U}{\partial V}\right)T = \frac{n^2 a}{V^2} \tag{32}$$

After integrating the above equation we will have:

$$\Delta U_{\text{Isothermal}} = \int_{V_1}^{V_2} \frac{n^2 a}{V^2} dV = n^2 a\left(-\frac{1}{V}\right) \tag{33}$$

In cold vapor transfer we always have $V_2 > V_1$, therefore:

$$\Delta U = n^2 a\left(\frac{1}{V_1} - \frac{1}{V_2}\right) \tag{34}$$

The constant T in ΔU indicates that the calculations can only be made in a small fragment of the pipeline. In the case of adopting small sections for a long pipeline in which the temperature is approximately constant, Eq. (34) can be written and ΔU can be determined.

3.2.2. Determination of enthalpy energy H

Now, it is attempted to reach the enthalpy H given the internal energy U and through the thermodynamic equations. For the enthalpy H, it has been shown that the second virial coefficient B, is related to the internal energy U and the following equation exists between the two energies H and U:

$$\Delta H = \Delta U + BP \tag{35}$$

The second virial coefficient is also associated with the van Der Waals coefficients (a, b).

$$B = b - \frac{n^2 a}{RT} \tag{36}$$

3.2.3. Determination of the Gibbs energy G

The next step is to calculate ΔG. The well-known Gibbs–Helmholtz equation allows for the relation of ΔG to ΔH.

$$\left(\frac{\partial\left(\frac{G}{T}\right)}{\partial T}\right)T = -\frac{\Delta H}{T^2} \tag{37}$$

Taking into account the pipe elements that are considered at the lowest length of the pipe, Eq. (38) can be used instead of Eq. (37). From the Gibbs–Helmholtz equation, both G/T and G can be calculated.

$$\left(\frac{\Delta\left(\frac{G}{T}\right)}{\Delta T}\right)P = -\frac{\Delta H}{T^2} \tag{38}$$

3.2.4. Determination of the entropy S

Now ΔS can be calculated at any section in the pipe. The best thermodynamic equation by which ΔS can be calculated is the universal Eq. (39).

$$\Delta G = \Delta H - T\Delta S \tag{39}$$

Therefore, ΔS will be calculated by the following equation.

$$\Delta S = \frac{\Delta H - \Delta G}{T} \tag{40}$$

3.2.5. Determination of Helmholtz energy A

Finally, the Helmholtz energy A can be calculated given the entropy changes ΔS.

$$\Delta A = \Delta U - T\Delta S \tag{41}$$

Eqs. (42) and (43) can be employed to calculate C_p and C_V, and graphically or by deriving, the specific heats C_p and C_V can be calculated for each segment of the pipe. Plotting the enthalpy H and the internal energy U along the entire path with respect to temperature variations and obtaining the average slope of the graph, the specific heats C_p and C_V can be accurately determined.

$$\Delta H = C_p \cdot \Delta T \tag{42}$$

$$\Delta U = C_V \cdot \Delta T \tag{43}$$

3.3. Calculation of thermodynamic functions for SAVP in a field study (Bandar Abbas–Genu Path)

Regarding field studies between two points that have the potential of SAVP implementation, two sub-atmospheric vapor transfer studies have been already presented for the Sanaa heights and the Al Qur'an heights (adjacent to the Red Sea) [13], in addition, now a 30 km distance between the Geno heights and Bandar Abbas coastal city as a domestic field case examined in this study. Therefore, all the knowns and unknowns of the SAVP method are presented in this section. Fluid transfer velocity, temperature, pressure, and density variation profiles of the vapor, along with thermodynamic energies, are the main unknowns whose results are discussed below. Fig. 5 illustrates the enthalpy changes with respect to temperature along the transfer path. As can be seen, enthalpy decreases with decreasing temperature along the path.

The changes in the internal energy U in terms of temperature along the transfer path are depicted in Fig. 6. As observed in this figure, the more internal energy is consumed by the vapor rise in the pipe. In other words, the content of the internal energy is often spent on vapor rising, decreasing pressure, and hence decreasing temperature.

Up to here, all 10 thermodynamic variables for the SAVP transfer line have been calculated and determined. The last one of these calculations is the computation for a relation that interrelates pressure and temperature by a differential equation. This equation is the Clapeyron equation that can be seen by Eq. (44). This equation is for determining the slope of the vapor pressure of a saturated fluid and consequently is related to that part of the pipe that vapor has approached or passed the superheated zone (i.e., in condensation zone where x drops from one and approaches to zero). This pressure drop is the main cause of fluid suction throughout the pipeline.

$$\frac{dP}{dT} = \frac{h^{\alpha} - h^{\beta}}{T\left(v^{\alpha} - v^{\beta}\right)} \tag{44}$$

If α and β designate the vapor and liquid phases respectively, the enthalpy difference of these two phases is equal to the vapor condensation enthalpy. Moreover, the molar volume of the vapor phase is dramatically greater than that of the liquid, therefore, the form of the Clapeyron equation will be transformed from Eq. (44) to an applicable equation [16].

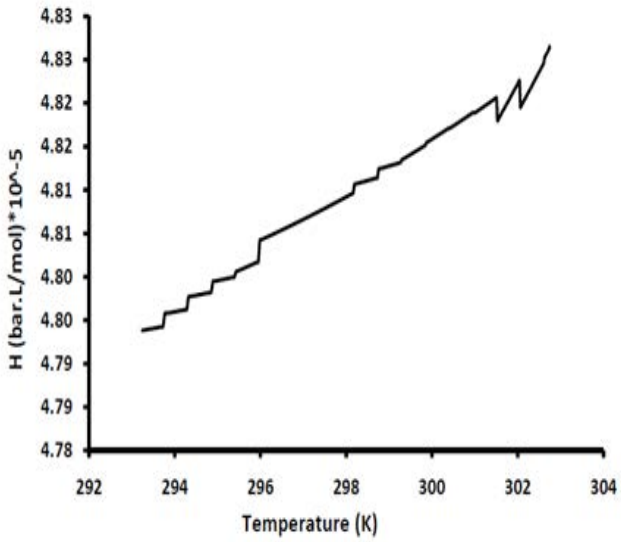

Fig. 5. Enthalpy changes in temperature in the process of desalination by the SAVP method.

$$\frac{d\left(\ln P\right)}{-d\left(\frac{1}{T}\right)} = \frac{\Delta h_{\text{Condensation}}}{R} \tag{45}$$

The Clapeyron equation actually expresses absolute pressure changes in terms of temperature during the phase change, and since these changes are expressed only in terms of temperature, the total derivative is used to write its differential equation and there is no need to use a partial derivative. Although the Clapeyron differential equation is applied for both condensation and evaporation, giving the link between the subjects with this paper, the Clapeyron equation could be used in this study only for condensation zone.

Although Fig. 4 shows temperature and pressure changes for the SAVP in both saturated and unsaturated paths, it does not explicitly indicate these changes in terms of path length (L). Therefore, Fig. 7 is presented to illustrate these changes in terms of the path length. This figure includes the behavior of the fluid temperature, pressure, density, and transfer rate in the unsaturated state with respect to the changes in the SAVP length. The insertion of data related to saturated vapor in Fig. 7 is not authorized because of their presence in thermodynamic tables; however, plotting the saturated vapor velocity (V_{sat}) to be compared with the hot vapor velocity (V_{sh}) and presenting its reasons are necessary from the point of view of the conversion of different types of energy (U, H, G, and A). For this reason, the saturated vapor velocity data are drawn in Fig. 7. In this figure, the temperature is expressed in Celsius degrees.

Fig. 7, as previously described, only involves vapor transfer and does not, of course, include the condensation length (L_C). The condensation length discussed earlier can be determined through empirical heat transfer relations and is therefore not a critical issue in the present study. Therefore, the components of the curves in Fig. 7 are only expressed until reaching the beginning of the condenser

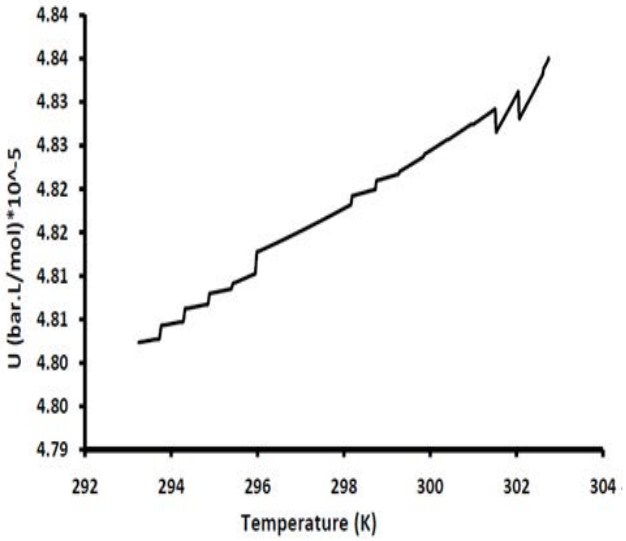

Fig. 6. Internal energy changes in temperature in the process of desalination by SAVP method.

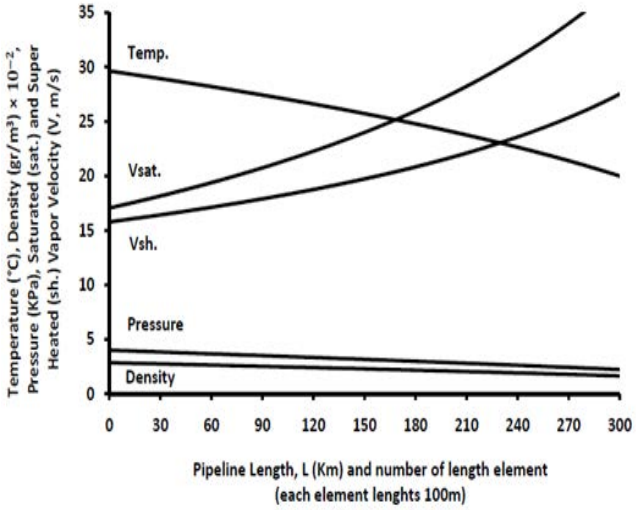

Fig. 7. Temperature, density, pressure, saturation vapor pressure, and superheated vapor velocity in the process of desalination by SAVP method.

and are discontinued there. The fluid pressure drop curve is one of the curves in Fig. 7 in which the pressure drops from about 3.99 to about 2.03 kPa. There is another important pressure drop that occurs based on Eq. (44) as defined in the Clapeyron relation. This pressure drop is attributed to the phase change in which the fluid density gradually increases due to the phase change to reach the liquid density. It is evident that the total pressure drop of the path (including the condensation length) is also affected by the pressure drop caused by the phase change.

The area enclosed by the graph in Fig. 8 is directly related to the difference between the two velocities of the vapor motion from the saturation path and motion in the

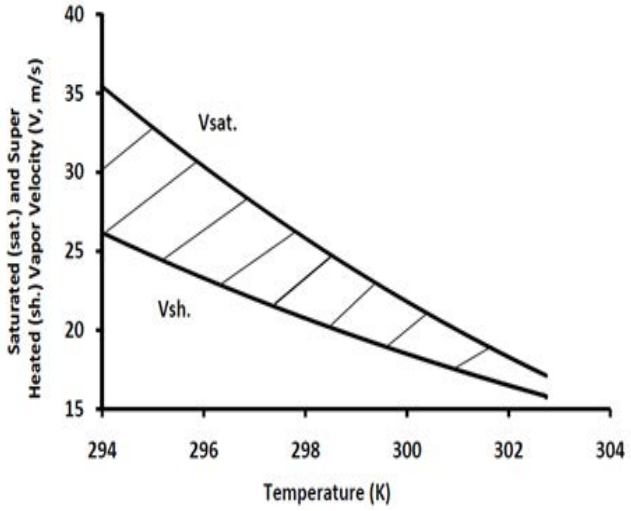

Fig. 8. Difference between two velocities of vapor motion from saturation path and hot zone.

superheated zone. In other words, the greater the difference between these two temperatures, the more significant the difference in SAVP velocities, in addition to increasing the difference between the saturated and unsaturated paths (hatched area in Fig. 8). In extreme cases, when the temperature difference between the hot and cold sources increases in short intervals in nature, severe storms occur at destructive speeds. This issue is reflected in the SAVP installation as a high vapor transfer velocity and motion of compressible fluids with Mach numbers near or even higher than one [17].

As it can be deduced from Fig. 8, the thermal energy content (ΔH) of the unsaturated path is higher than the thermal energy of the saturated path due to lying in the range of higher temperatures. Under the law of conservation of energy and conversion of energy from one form to another, in fact, the unsaturated path will inevitably occur at a slower speed (Fig. 8) for the SAVP because of a higher temperature, and this is quite logical and explainable. If the difference between the saturation temperature and the hot vapor temperature, such as the velocity of the saturated vapor and the hot vapor given in Fig. 8, is shown for the path, Fig. 9 will emerge.

It is not up to the user to select the SAVP motion from the saturated and unsaturated paths, and all SAVP paths pass through the unsaturated temperature path under any conditions with any initial assumption for warm and cold temperatures. Therefore, the introduction of the saturation path and its thermodynamic and dynamic properties is applied only as a starting point for calculations and for better understanding of the cold vapor transfer phenomenon. Given the review of the thermodynamic functions in the set of Eqs. (25)–(41), the functions of the thermal energy H, Gibbs energy G, Helmholtz energy A, and internal energy U can be calculated and represented. Fig. 10 illustrates the variations of these four energies in terms of the length variable. As it can be seen, the thermal energy H and the Helmholtz energy A decrease along the cold vapor transfer

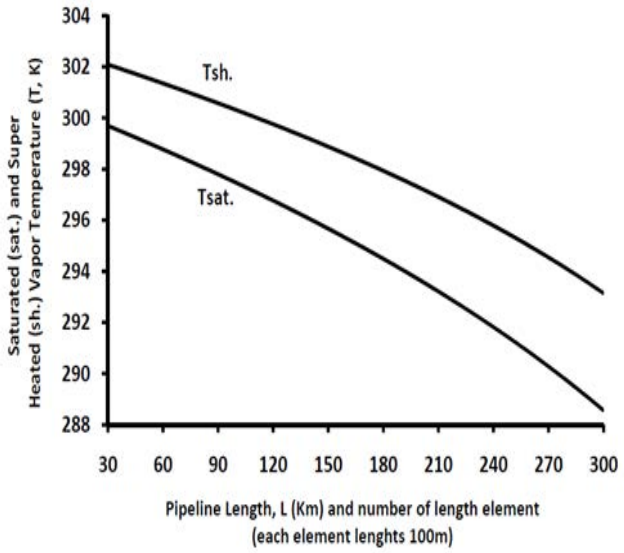

Fig. 9. Difference between two temperatures of vapor motion from saturation path and hot zone.

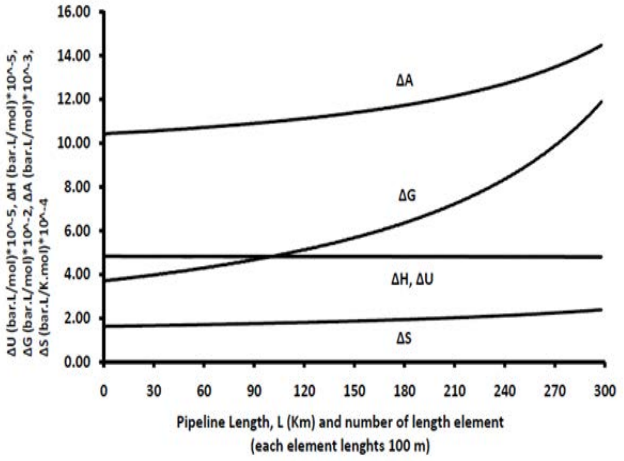

Fig. 10. Changes in heat energy functions H, Gibbs energy G, Helmholtz energy A, and internal energy U in variable length.

paths, and the Gibbs energy G, internal energy U, and the thermodynamic variable of the entropy S increase.

According to Eq. (45) and based on the vapor table (available in thermodynamic textbooks [16]), the enthalpy at the beginning and at the end of the condensation length at 20°C and 5°C equals 4.42 × 105 and 4.48 × 105 L bar/mol, respectively. Therefore, as it was already known, the phase change enthalpy is not strongly dependent on temperature, and in almost a large range of temperatures, it experiences little change.

After the inclusion of temperature, pressure, density, and thermodynamic functions (for the four energies) and determining the actual transfer velocity (unsaturated state or hot vapor) and the assumed transfer velocity (saturation state) in the SAVP, the vapor transfer path can be presented in full thermo-physic and thermodynamic details and the results can be used in future studies. What is considered for the development of SAVP knowledge is the study of this phenomenon in the dynamic state in which the hot and cold source temperatures and the thermal conditions of the SAVP path are subject to inherently time-dependent factors. In such a case, new, and interesting arguments arise that will be deferred to other studies. This issue begins from the review and simplification of the basic energy equation and its thermodynamic background is based on the NET principles that can be solved using advanced mathematics including the use of the Green's function. It is worth noting that the area under the graph of Fig. 8 is directly proportional to the vapor transfer flow rate, or SAVP discharge. The higher temperature difference results in a wider area under the graph and consequently more vapor flows along the SAVP path. Fig. 8 can also be plotted for enthalpy of the saturation and hot vapor paths. The area under the graph indicates the difference between the two enthalpies, one derived from the vapor table ($H^{\text{sat}}_{(T,P)}$) and the other from the calculations of this study ($H^{\text{SH}}_{(T,P)}$), with an appropriate coefficient ($h(T,P)$), which is applied to convert this difference into the transferrable vapor volume, enabling the user to calculate the SAVP volume flow rate.

$$S = \int_{T_1}^{T_2} h(T,P)\left(H^{\text{SH}}_{(T,P)} - H^{\text{Sat}}_{(T,P)}\right)dT = F_{\text{SAVP}} = \bar{V} \times A \tag{46}$$

where T_1, T_2, $\bar{V}$, and A are the hot source temperature, the cold source temperature, the average velocity along the path, and the hatched surface area, respectively. Specific heats at constant pressure (C_P) and constant volume (C_V) can be calculated directly from dividing the enthalpy and internal energy of each fragment of the pipe by the temperature of that fragment. The point obtained from thermodynamic calculations indicates that the energy equivalent to the temperature–entropy product (TS) has much more drastic changes than the energy equivalent to the pressure–volume product (PV). The almost identical values of the calculated enthalpy and the internal energy, as well as the significant difference between the Gibbs energy and the enthalpy confirm this fact.

4. Conclusion

It is not up to the user to select the SAVP motion from the saturated and unsaturated paths, and all SAVP paths pass through the unsaturated temperature path under any conditions with any initial assumption for the hot and cold temperatures. Therefore, the introduction of the saturation path and its thermodynamic and dynamic properties is applied only as a starting point for calculations and for a better understanding of the cold vapor transfer phenomenon. In this study, based on the thermodynamic functions, the functions including the thermal energy H, the Gibbs energy G, the Helmholtz energy A, and the internal energy U were calculated and shown in terms of the length variable. Fluid transfer along the path is caused by the pressure difference between the two hot and cold sources, and the pressure drop causing the movement is the sum of the fluid pressure drop along the path and the pressure drop at the condensation point due to phase change. The thermodynamic functions

introduced in this study enable the user to calculate the four thermodynamic energies, temperature, pressure, number of moles, specific volume, specific density, entropy, and vapor velocity at any point of the vapor transfer path. The above data are the basis for the design and implementation of the desalination system through SAVP.

Acknowledgments

We gratefully acknowledge the helps and assistance of Mr. Koosha Aghazadeh, for his cooperation in math and computer programming. Koosha is a graduate student from the School of Civil Engineering, University of Tehran, Iran.

Symbols

α_w	—	Water activity equal to water concentration, mol/L
A or ΔA	—	Helmholtz energy (1.04–1.45) × 10^3, L bar/mol
C_P	—	Specific heat capacity (at cons. P) could be calculated by ΔH, L bar/mol K
C_V	—	Specific heat capacity (at cons. V) could be calculated by ΔU, L bar/mol K
D	—	Diameter of pipe 2, m
f	—	Friction factor 0–0.1, DL*
g	—	Acceleration due to gravity 9.81, m/s^2
G or ΔG	—	Gibbs energy (3.7–11.9) × 10^2, L bar/mol
H	—	Difference in elevation; height 2,300, m
H or ΔH	—	Enthalpy (4.79–4.83) × 10^5, L bar/mol
L	—	Length of transport part 30, km
P	—	Pressure or pressure drop up to 150, kPa
R	—	Universal gas constant 0.083144, L bar/mol K
S or ΔS	—	Entropy (1.6–2.39) × 10^4, L bar/mol K
T or ΔT	—	Temperature 293.15–303.15, K
U or ΔU	—	Internal energy (4.80–4.84) × 10^5, L bar/mol
V	—	1/Thermodynamic water density 0.017–0.018, L/mol
V	—	Vapor velocity 15–38, m/s

Greek

α	—	Pipeline slope arc tan (H/L) = arc tan 0.766, DL
γ	—	Activity coefficient for species up to 1, DL
$\gamma^{\pm}$	—	Mean ionic activity coefficient up to 1, DL
μ	—	Water viscosity (liquid) (0.798−1.519) × 10^{-3}, Pa s
ρ	—	Water density (liquid) 996−1,000, kg/m^3
ρ_t	—	Thermodynamic water density (L) 55.33–55.56, mol/L
ϕ	—	Osmotic coefficient (for water) up to 1, DL

DL = dimensionless

References

[1] K.S. Pitzer, Activity Coefficients in Electrolyte Solutions, 2nd ed., Chapter 6, CRC Press, London, 1991.
[2] R. Feistel, A new extended Gibbs thermodynamic potential of seawater, Prog. Oceanogr., 58 (2003) 43–114.
[3] M.H. Sharqawy, J.H. Lienhardand, S.M. Zubair, Thermophysical properties of seawater: a review of existing correlations and data, Desal. Water Treat., 16 (2010) 354–380.
[4] R. Feistel, Thermodynamic properties of seawater, ice and humid air: TEOS-10, before and beyond, Ocean Sci., 14 (2018) 471–502.
[5] T. Younos, K.E. Tulou, Overview of desalination techniques, J. Contemp. Water Res. Edu., 132 (2005) 3–10.
[6] N. El-Haddad, H. Yared, R. Carbonell, Energy Efficient Desalination: Meeting the GCC's Water Needs in an Environmentally Sustainable Way, International Water Summit (IWS), Environment Agency Abu Dhabi, Sourced and Reported #4, 2018.
[7] M.S. Wiener, B.V. Salas, A. Eliezer, Corrosion control in the desalination industry, Adv. Mater. Res., 95 (2011) 71–86, doi: 10.4028/www.scientific.net/AMR.95.29.
[8] A. Del Amo, P. Antonio, System and Method for Desalinating Seawater, Patent WO/171986 A1, 2012.
[9] M.E. Kazemian, A. Bezadmehr, S.M.H. Sarvari, Thermodynamic optimization of multi-effect desalination plant using the DoE method, Desalination, 257 (2010) 195–205.
[10] J. Al-Zahrani, J. Orfi, Z. Al-Suhaibani, B. Salim, H. Al-Ansary, Thermodynamic analysis of reverse osmosis desalination unit with energy recovery system, Procedia Eng., 33 (2012) 404–414.
[11] M.G. Abdoelatef, R.M. Field, L. Yong-Kwan, Thermodynamic evaluation of coupling APR1400 with a thermal desalination plant, Chem. Mol. Eng., 9 (2015) 1278–1286.
[12] K. Mistry, R. McGovern, G. Thiel, E. Summers, S. Zubair, J. Lienhard, Entropy generation analysis of desalination technologies, Entropy, 13 (2011) 1829–1864.
[13] W. Wagner, A. Pruß, The IAPWS formulation 1995 for the thermodynamic properties of ordinary water substance for general and scientific use, J. Phys. Chem. Ref. Data, 31 (2002) 387–533.
[14] K. Inoue, Y. Abe, M. Murakami, T. Mori, Feasibility study of desalination technology utilizing the temperature difference between seawater and inland atmosphere, Desalination, 197 (2006) 137–153.
[15] M.F. Anderson, Sub-Atmospheric Pressure Desalination and/or Cooling Method and Means, Patent US/4366030, 1982.
[16] J.M. Smith, H.C. Van Ness, M.M. Abbott, Introduction to Chemical Engineering Thermodynamics, 7th ed., McGraw-Hill Education, California, USA, 2004.
[17] P.H. Oosthuizen, W.E. Carscallen, Compressible Fluid Flow, Chapter 9, McGraw Hill Companies Incorporation, New York, NY, 1997.